

## Article

# Optimal Sequencing of Arrival Flights at Metroplex Airports: A Study on Shared Waypoints Based on Path Selection and Rolling Horizon Control

Furong Jiang <sup>1,2</sup>  and Zhaoning Zhang <sup>2,3,\*</sup><sup>1</sup> Flight Academy, Civil Aviation University of China, Tianjin 300300, China; frjiang@cauc.edu.cn<sup>2</sup> College of Safety Science and Engineering, Civil Aviation University of China, Tianjin 300300, China<sup>3</sup> College of Air Traffic Management, Civil Aviation University of China, Tianjin 300300, China

\* Correspondence: zzhaoning@263.net

**Abstract:** The civil aviation industry is experiencing significant growth in air traffic density within terminal areas, necessitating improved air traffic efficiency. In China's pursuit of world-class airport clusters, operational complexities arise due to the co-location of these airports in the same terminal area airspace, resulting in lower operational efficiency. To mitigate congestion and flight delays, this study proposes an integrated model that considers multiple runways and route selections, accounting for actual route point restrictions. Utilizing actual operational data from Shanghai metroplex, the proposed model is validated. The study focuses on the airport metroplex system and presents a comprehensive mixed-integer programming (MIP) model for arrival sequencing, considering multiple airports, runways, and routes. The maximum landing efficiency is adopted as the objective function, optimizing arrival scheduling while considering time intervals, route selection, and landing constraints. The Multi-waypoint Rolling Horizon Control (MWRHC) algorithm is employed to tackle time-efficiency challenges, ensuring flight safety by continuous monitoring of flights in the terminal area. Comparative analysis reveals the algorithm's superior optimization performance for single-runway airports compared to dual-runway airports. Overall, the proposed model and algorithm effectively improve the efficiency of multi-airport arrival scheduling in airport metroplex systems.

**Keywords:** airport metroplex; flight optimal sequencing; mixed-integer programming (MIP); rolling horizon control (RHC)



**Citation:** Jiang, F.; Zhang, Z. Optimal Sequencing of Arrival Flights at Metroplex Airports: A Study on Shared Waypoints Based on Path Selection and Rolling Horizon Control. *Aerospace* **2023**, *10*, 881. <https://doi.org/10.3390/aerospace10100881>

Academic Editor: Cheng-Lung (Richard) Wu

Received: 15 September 2023

Revised: 10 October 2023

Accepted: 11 October 2023

Published: 12 October 2023



**Copyright:** © 2023 by the authors. Licensee MDPI, Basel, Switzerland. This article is an open access article distributed under the terms and conditions of the Creative Commons Attribution (CC BY) license (<https://creativecommons.org/licenses/by/4.0/>).

## 1. Introduction

### 1.1. Background

As the civil aviation industry continues to evolve steadily, the density of air traffic within terminal areas is rising markedly. With this increasing complexity in traffic flow, the quest for improved air traffic efficiency has become pivotal in enhancing the operational efficacy of terminal areas. China is vigorously advancing the construction of world-class airport clusters. However, the operation of these airport clusters, which are also known as “airport metroplex”, is coupled and complex, largely due to their co-location within the same terminal area airspace [1–3]. The mutual influence among these airports and their shared use of airspace resources inevitably lead to lower operational efficiency [4–7].

At airport metroplex, the close proximity of various airports often results in multiple flights having the same trajectory towards their respective destinations, essentially sharing the same waypoints. Currently, each airport tends to manage its flight schedules independently, leading to congestion at these shared waypoints. These shared waypoints are key nodes, which serve a crucial role in connecting inbound and outbound traffic. Research conducted by frontline units indicates that optimizing and coordinating traffic flow at these

shared waypoints within a group of metroplex airports can significantly reduce operational congestion and flight delays.

### 1.2. Literature Review

In recent decades, several studies on the optimization problem of inbound flight sequencing have been conducted, with a primary focus on individual airports. In 2010, Mesgarpour et al. [8] developed a model that fulfills the requirements of air traffic controllers, airports, airlines, and governments by minimizing average delay, maximizing runway throughput, and reducing fuel costs as objectives, considering the constraints of wake vortex safety spacing, arrival time windows, and airline priority levels. In 2013, Hancerliogullari et al. [9] proposed a new mixed-integer programming model for flight scheduling, which aimed at minimizing total weighted delay time, and in addition to considering wake vortex spacing and arrival time window constraints, it also incorporated runway load balancing constraints. In 2014, Sölveling et al. [10] proposed a stochastic branch-and-bound-based algorithm to develop the optimal or near-optimal solution of stochastic airport runway scheduling problems. In the same year, Ma Yuanyuan et al. [11] established a collaborative scheduling model for approach flights in multi-airport terminal areas, taking into account such interval constraints as control handover, wake flow and multi-runway operation. Wang Lili et al. [12] used the double-coding genetic algorithm to establish a parallel runway approach and departure flight sequencing model including cargo flights, effectively reducing flight delays.

In order to schedule approach flights more efficiently, it is necessary to consider the route selection and the arrangement of restricted airspace resources within the airport metroplex. Sidiropoulos et al. [13] proposed a sorting optimization strategy for airport metroplex inbound and outbound flights in 2015. Firstly, inbound and outbound flights were clustered to obtain dynamic paths according to their temporal and spatial distribution; secondly, dynamic paths were prioritized; finally, dynamic path flight sorting based on optional waypoints was realized on the premise of ensuring flight intervals. In 2019, Zhang Zhaoning et al. employed a multi-objective planning approach to devise an airport group flow allocation strategy centered on capacity flow matching [14]. This strategy was formulated to address the challenges associated with airport group flight delays and air traffic congestion. In 2020, Yin et al. [15] proposed a runway allocation and ranking method focusing on the utilization of multiple airports and multiple runways in an airport group based on the impact of runway configurations of airports in an airport group on traffic flow management. Liu Jixin et al. [16] designed an elite retention genetic algorithm and a fast non-dominated sorting genetic algorithm with elite strategy, and established a collaborative approach flight sorting model based on air traffic density. In 2021, aiming at the common waypoints of multi-airport coupled operation, Wang Lili et al. [17] introduced a penalty factor and employed the minimum total delay time cost as the objective function to establish a flight optimization ranking model based on the sliding time window algorithm and particle swarm optimization algorithm. In 2022, Wei Ming et al. proposed an optimization model for flight entry and departure scheduling, considering aspects such as runway invasion and potential risk level, thereby broadening the scope of application scenarios for flight scheduling models [18,19].

Most of the established models prioritize minimizing total delay cost or minimizing delay time as their objective function, taking into account runway allocation models constrained by wake vortex safety intervals and arrival time windows. Models addressing route selection and specific route point restrictions are relatively scarce, and studies considering current route selection and specific route point restrictions often fail to fully reflect the reality of terminal areas. In terms of scheduling methods, the first come, first served (FCFS) principle is widely adopted; for runway assignment, proximity in the air is typically prioritized. While such methods are easy to operate, they can lead to wastage of airspace resources and imbalance in runway resource utilization when the airspace is crowded, causing flight delays.

### 1.3. Contribution of the Research

To address these issues, this paper proposes an integrated model that considers multiple runways and multiple route selections, and accounts for actual route point restrictions. As for model solution, a targeted rolling time domain control solution algorithm is put forward. For practical validation, actual operational data from multiple terminal areas of Shanghai metroplex are used.

## 2. Methodology

### 2.1. Problem Description

The difference between a metroplex and a single airport is mainly due to the coupling and complexity of its operation. The operation of each airport in a metropolitan region is highly correlated, and the allocation of time and space resources cannot be considered independently, but should be considered from the perspective of overall operation. The shared waypoint is the public resource of the metroplex airspace, which has a certain impact on the entire system of the metroplex, and is closely connected with the terminal area and other airspace. Improving the operation efficiency of the shared waypoint is the key to enhance the global resources of the metroplex system. Therefore, this paper studies the scheduling of flights through shared waypoints of airport groups. The planned crossing time of flights taking off from each airport is known, and the traffic flow of shared waypoints is effectively optimized and allocated to obtain a reasonable crossing order and crossing time.

### 2.2. Modeling

#### 2.2.1. Parameters

Before delving into the various parameters employed in our study, it's essential to define the sets and the parameters that form the basis of our model. Tables 1 and 2 provide a clear breakdown of these sets and parameters along with their definitions.

**Table 1.** Definitions for sets.

Set Symbol	Definition	Index Symbol
$A$	set of airports in metroplex	$a$
$F$	set of arrival flights	$i, j$
$F_a$	set of flights landing at airport $a$	
$R$	set of routes available	$r, s$
$R_i$	set of routes available for flight $i$ , $i \in F$ , $R_i \subset R$	
$D$	set of segments that make up available routes	$d$
$D_r$	set of segments that make up route $r$	
$P$	set of waypoints in metroplex	$p$
$P_r$	set of waypoints in route $r$	
$W$	set of runways in metroplex airports, $W \subset P$	$w$
$W_a$	set of runway(s) available for airport $a$	
$SA$	set of scheduled arriving time of flights	

**Table 2.** Definitions for parameters.

Symbol	Definition
$Tmi_d$	the minimum flying duration for segment $d$
$ps_d$	the start waypoint of segment $d$
$pe_d$	the end waypoint of segment $d$
$E_{ip}^r$	the earliest time for flight $i$ arriving at waypoint $p$ with choosing route $r$
$L_{ip}^r$	the latest time for flight $i$ arriving at waypoint $p$ with choosing route $r$

**Table 2.** Cont.

Symbol	Definition
$S_{ij}$	the minimum time interval for wake turbulence purposes that must be satisfied when flight $i$ and flight $j$ are on the same runway of one airport
$s_{ij}$	the minimum time interval for wake turbulence purposes that must be satisfied when flight $i$ and flight $j$ are on different runways of one airport
$T_{ij}$	the minimum safe interval between flight $i$ and flight $j$ when operating under radar control
$K$	maximum position shifting (MPS) value
$M$	a very large number
$N$	the total flight number
$N_a$	the number of flights landing at airport $a$
$\delta_{if}^a$	$\begin{cases} 1, & \text{if flight } i \text{ is at position } f \text{ in the FCFS sequence of airport } a \\ 0, & \text{otherwise} \end{cases}$

2.2.2. Decision Variables

To make effective decisions in our model, certain decision variables are incorporated. Table 3 provides a comprehensive overview of these decision variables and their definitions.

**Table 3.** Definitions for decision variables.

Symbol	Definition
$AT_{ip}$	the simulated time that flight $i$ arriving through waypoint $p$
$ALT_i$	the simulated landing time of flight $i$
$x_i^r$	$\begin{cases} 1, & \text{if flight } i \text{ choose route } r \\ 0, & \text{otherwise} \end{cases}$
$\alpha_{ijp}$	$\begin{cases} 1, & \text{if flight } i \text{ passing through waypoint } p \text{ before flight } j \\ 0, & \text{otherwise} \end{cases}$
$z_{ij}$	$\begin{cases} 1, & \text{if flight } i \text{ landing before flight } j \\ 0, & \text{otherwise} \end{cases}$
$\gamma_i^w$	$\begin{cases} 1, & \text{if flight } i \text{ landing at runway } w \\ 0, & \text{otherwise} \end{cases}$

2.2.3. Objective Function

To enhance efficiency while upholding safety standards, the objective function is formulated from the perspective of air traffic flow management. This function seeks to minimize the last landing flight time within the optimized time period, thereby maximizing the operational efficiency of each airport runway.

Objective:  $\min \max ALT_i$

2.2.4. Constraint Conditions

Assuming that flight  $i$  corresponds to its target airport  $a$ . The constraint conditions, which are integrally based on the parameters and decision variables delineated in Tables 1–3, are provided in Table 4.

**Table 4.** Constraint Conditions.

Constraints	No.
$\sum_{r \in R_i} x_i^r = 1, \forall i \in F$	(1)
$\sum_{w \in W_a} \gamma_i^w = 1, \forall i \in F$	(2)
$\gamma_i^w = 1, \text{ if } w \in P_r \text{ and } x_i^r = 1$	(3)
$AT_{iw} - M(1 - x_i^r) \leq ALT_i \leq AT_{iw} + M(1 - x_i^r), \forall i \in F; r \in P_r \cap W_a$	(4)

**Table 4.** Cont.

Constraints	No.
$z_{ij} + z_{ji} = 1, \forall i \neq j \in F$	(5)
$\sum_{r \in R_i} x_i^r E_{ip}^r \leq AT_{ip} \leq \sum_{r \in R_i} x_i^r L_{ip}^r, \forall i \in F; \forall p \in P$	(6)
$AT_{i,pe_d} - AT_{i,ps_d} \geq Tmid - M \cdot (1 - x_i^r), \forall i \in F; \forall d \in D_r$	(7)
$AT_{ip} - AT_{jp} \geq T_{ij} - M \cdot (1 - \alpha_{ijp}), \forall i \neq j \in F; \forall p \in P - W$	(8)
$ALT_i - ALT_j \geq S_{ij} \cdot \gamma_i^w \gamma_j^w + s_{ij} \cdot (1 - \gamma_i^w \gamma_j^w) - M \cdot (1 - z_{ij}), \forall i \neq j \in F; \forall p \in P - W$	(9)
$\alpha_{ijp} + \alpha_{jip} \leq 2 - x_i^r - x_j^s, \forall i \neq j \in F; \forall r \in R_i; \forall s \in R_j; \forall p \in P - P_r \cap P_s$	(10)
$x_i^r + x_j^s - 1 \leq \alpha_{ijp} + \alpha_{jip} \leq, \forall i \neq j \in F; \forall r \in R_i; \forall s \in R_j; \forall p \in P_r \cap P_s$	(11)
$\sum_{w \in W_a} \alpha_{ijw} \leq z_{ij}, \forall i \neq j \in F$	(12)
$\sum_{j \in F \setminus \{i\}} z_{ji} + 1 - \sum_{f=1}^{N_d} f \cdot \delta_{if}^d \geq -K, \forall i \in F$	(13)
$\sum_{j \in F \setminus \{i\}} z_{ji} + 1 - \sum_{f=1}^{N_s} f \cdot \delta_{if}^s \leq K, \forall i \in F$	(14)

Constraints (1)–(3): Each flight is assigned one unique route and lands on only one runway. This ensures that there are no conflicts in the landing sequence and that every flight has a clear and unique path to follow. This fundamental constraint is rooted in the premise of ensuring flight safety and operational efficiency, as discussed by Faye [20].

Constraint (4): The runway is always the last waypoint on a flight’s route. The time of arrival at this waypoint signifies the flight’s actual landing time. This constraint guarantees a seamless and logical progression of a flight’s path, ensuring that once a flight reaches its final waypoint, it is indeed on the ground, as derived from Pawelek et al. [21].

Constraint (5): This constraint ensures the uniqueness of the order between two aircrafts. Specifically, it dictates that if flight *i* precedes flight *j*, then flight *i* cannot subsequently be found trailing behind flight *j*.

Constraint (6): This represents time window constraints, ensuring flights pass through each waypoint within a specific timeframe. By enforcing this, the model ensures that flights adhere to their scheduled flight paths and timings, reducing the potential for air traffic congestion or conflicts. Time window constraints, particularly in dense airspaces, are essential to maintaining a steady flow of traffic [21,22].

Constraint (7): This constraint guarantees that the time duration for a flight to traverse between two consecutive waypoints is no less than the minimum flying duration established for that segment. Essentially, it ensures that flights do not pass through these waypoints faster than safety and operational guidelines permit.

Constraint (8): Flights arriving at the same waypoint (excluding runways) must meet the radar control safety interval. This constraint ensures that flights are adequately spaced out when they converge at common waypoints, reducing the risk of conflicts and ensuring smooth transitions from one waypoint to the next.

Constraint (9): This focuses on the actual landing times of two flights on the runways of the same airport. The time intervals between these landings must meet wake turbulence separation criteria. Wake turbulence from a leading aircraft can be hazardous for the trailing one, especially during landing phases. Adhering to these intervals, as derived from prior research [21], ensures safe landings by preventing potential wake turbulence incidents.

Constraints (10)–(12): These constraints enforce logical consistency regarding the order in which flights pass through waypoints. If two flights traverse a particular waypoint, their order must be unique, preventing ambiguity in sequencing and reducing the possibility of conflicts at these waypoints.

Constraints (13) and (14): These introduce the constrained position shifting (CPS) constraint, stating that a plane cannot shift by more than  $K$  positions from its original first come, first served (FCFS) position  $\delta_{if}^a$ . This constraint ensures that while optimizing flight sequences, the solution remains relatively close to the initial order to avoid drastic changes that might overwhelm air traffic controllers or lead to logistical challenges.

2.3. Algorithm

For the flight sequencing of multi-shared waypoints in a metropolitan region, this paper uses a Multi-waypoint Rolling Horizon Control (MWRHC) algorithm based on RHC [23], which is presented in Figure 1. The rolling horizon control (RHC) strategy divides the entire planning horizon into a series of overlapping windows. Each window spans a duration of  $3T$ , and with each iteration, the window advances by a duration of  $T$ . As in the example shown in Figure 2, there are 5 enter points (EPs), the start waypoints of the route into the metropolitan region; 12 middle points (MPs), and 6 final point (FPs).

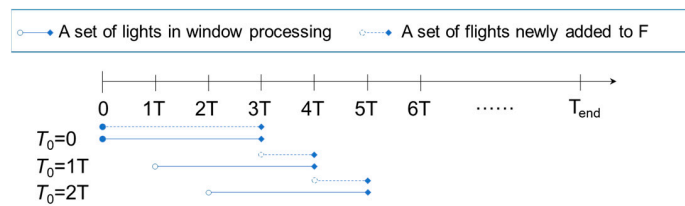


Figure 1. Window processing in rolling horizon framework when sliding window size is  $3T$  and step size is  $T$ .

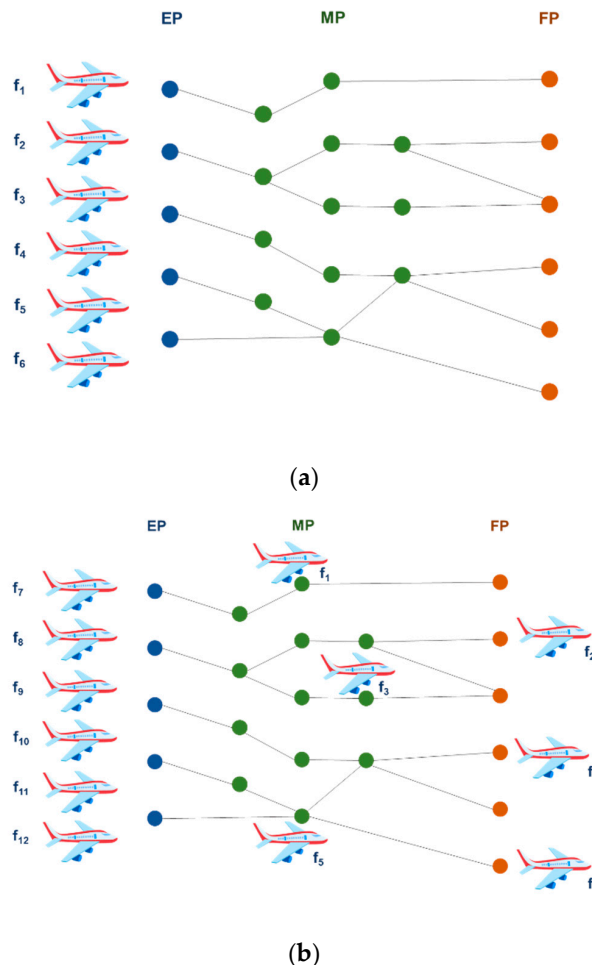


Figure 2. Schematic diagram of the 1st (a) and 2nd (b) horizons of MWRHC.

**Initialization Phase:** At the start ( $T_0$ ), the initial window covers the interval  $[T_0, T_0 + 3T]$ . During this phase, optimization is performed considering all flights expected to pass the enter points (EPs) within this window, as presented in Figure 2a.

**Rolling Phase:** As time progresses, the window slides forward by  $T$ . For instance, at time  $T_0 + T$ , the window covers the interval  $[T_0 + T, T_0 + 4T]$ . The optimization process is repeated considering updated flight data and schedules.

**Data Update:** With each window slide, the flight optimization queue is updated. This involves removing flights that were already simulated as having landed in the previous window, and incorporating new flights expected to pass the EP in the current window, as illustrated in Figure 2b. Concurrently, the current waypoint of each flight and the estimated time of passing through the previous waypoint are updated to reflect real-time adjustments and deviations.

The pseudo-code of the above MWRHC algorithm is listed as Algorithm 1.

---

**Algorithm 1.** Pseudo-code for MWRHC

---

```

Step 1: Initialize variables and data structures,  $h = 1$ 
Step 2: Calculate the expected arrival time window for each flight to reach each waypoint on the
available route selected
    while  $h < H$ :
Step 3: Initialize the optimization queue and variable set for the optimization time domain  $h$ 
Create empty list  $F\_h[h]$ 
Step 4: Add flights with expected passing EP time within  $[T_0, T_0 + NT]$  to the optimization
queue  $F\_h$ 
for each  $flight\_id, flight\_data$  in  $F$ :
    if  $flight\_data['starttime']$  is in  $range(T_0, T_0 + NT)$ :
        Append  $flight\_id$  to  $F\_h[h]$ 
Step 5: Solve the mixed-integer programming (MIP) model and update the selected routes and
flight status
subProblem = create_subProblem( $F\_h\_dict$ , routes, airport_runway)
subProblem.optimize()
update_selected_routes(subProblem, selected_routes)
update_flight_status( $F\_h\_dict$ , selected_routes)
Step 6: Check the flight status of the flights in  $F\_h$  (landed or not) and if the flight has not
landed before  $T_0 + T$ , update the entry point and output the actual arrival time before the point
update_waypoint_information( $F\_h\_dict$ , selected_routes)
Step 7: Update  $T_0$  and  $h$ 
 $T_0 = T_0 + T$ 
 $h = h + 1$ 
Step 8: Calculate expected arrival time window for each waypoint
Step 9: Update the optimization queue  $F\_h$ 
Step 10: Merge the current  $F\_h\_dict$  with the previous  $F\_h\_dict$ 

```

---

### 3. Experimentation

#### 3.1. Data Description

The Yangtze River Delta Airport Metroplex, which is also called Airport Cluster, is one of the four world-class airport clusters in China. The major airport identifier and corresponding names are listed in Table 5. The main waypoints and waypoint numbers of the arrival routes of the six airports in the airport metroplex are shown in Figure 3. To facilitate empirical research, this study presents a comprehensive compilation of optional arrival routes and landing runways, each assigned a unique numerical identifier. These encompass the entry waypoint within the metropolitan region, the waypoints of the arrival, and the landing runways, collectively referred to as “arrival routes”. For a detailed representation of the specific flight routes and the available routes for each airport based on real flight route information for 2019, please refer to Tables 6 and 7.

**Table 5.** Major airports name of Yangtze River Delta Airport Metroplex.

Airport Identifier	Airport Name
NKG	Nanjing Lukou
SHA	Shanghai Hongqiao
PVG	Shanghai Pudong
WUX	Wuxi Shuofang
HGH	Hangzhou Xiaoshan
NGB	Ningbo Lishe

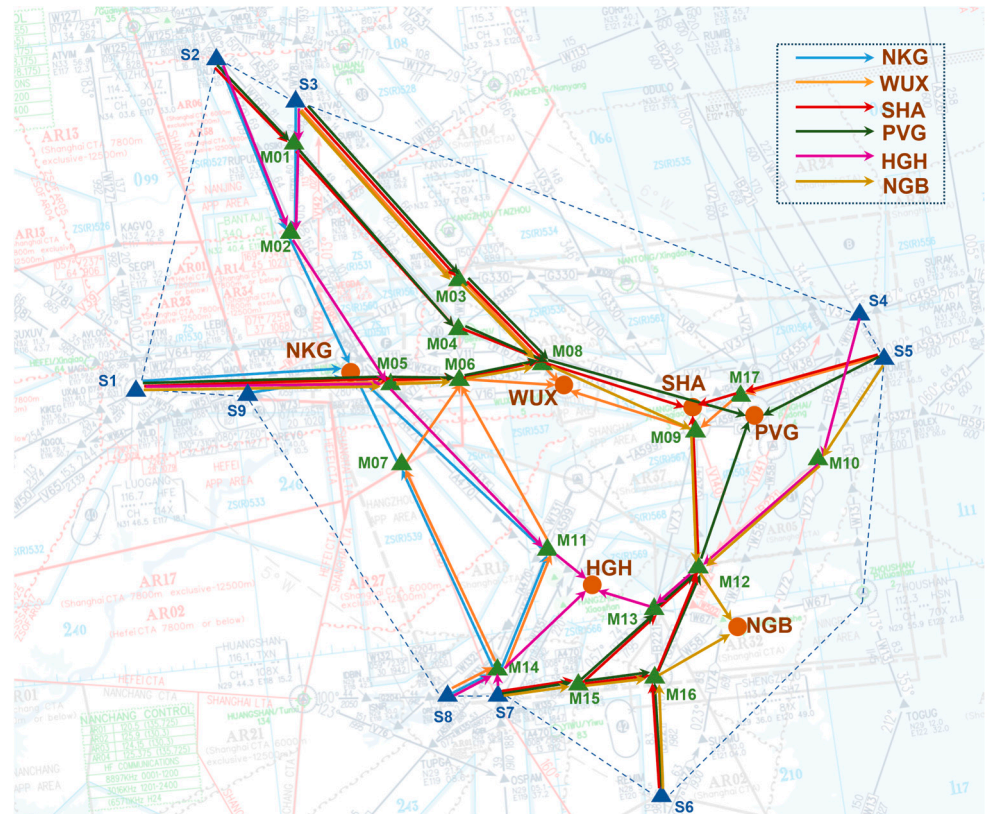


**Figure 3.** Distribution of Major Waypoints (M01–M17) along Arrival Routes in the Yangtze River Delta Airport Metroplex Region (the area surrounded by dot lines).

**Table 6.** Available routes for arrival flights in Yangtze River delta metropolitan region.

Start Point	Route no.	Waypoints
S1	01	S1-NKGR
	02	S1-M05-M06-M08-SHAR
	03	S1-M05-M06-M08-PVGR1
	04	S1-M05-M06-M08-PVGR2
	05	S1-M05-M06-WUXR
	06	S1-M05-M11-HGHR
	07	S1-M05-M06-M08-M09-M12-NGBR
S2	08	S2-M02-NKGR
	09	S2-M01-M04-M08-SHAR
	10	S2-M01-M04-M08-PVGR1
	11	S2-M01-M04-M08-PVGR2
	12	S2-M02-M05-M11-HGHR

**Table 6.** *Cont.*

Start Point	Route no.	Waypoints	
S3	13	S3-M01-M02-NKGR	
	14	S3-M01-M08-SHAR	
	15	S3-M03-M08-PVGR1	
	16	S3-M03-M08-PVGR2	
	17	S3-M03-WUXR	
	18	S3-M01-M02-M05-M11-HGHR	
	19	S3-M03-M08-M09-M12-NGBR	
	S4	20	S4-M10-M12-M13-HGHR
		S5	21
22	S5-PVGR1		
23	S5-PVGR2		
24	S5-M17-M09-WUXR		
25	S5-M10-M12-NGBR		
S6	26		S6-M16-M12-SHAR
	27	S6-M16-M12-PVGR1	
	28	S6-M16-M12-PVGR2	
	29	S6-M16-NGBR	
S7	30	S7-M15-M13-M12-SHAR	
	31	S7-M15-M16-M12-SHAR	
	32	S7-M15-M13-M12-PVGR1	
	33	S7-M15-M16-M12-PVGR2	
	34	S7-M15-M13-M12-PVGR1	
	35	S7-M15-M16-M12-PVGR2	
	36	S7-M14-HGHR	
	37	S7-M15-M16-NGBR	
S8	38	S8-M14-M11-NKGR	
	39	S8-M14-M07-NKGR	
	40	S8-M14-M11-M06-WUXR	
	41	S8-M14-M07-M06-WUXR	
	42	S8-M14-HGHR	
S9	43	S9-NKGR	

**Table 7.** Optional arrivals route codes for each airport.

Landing Airport	Route No.
NKG	01, 08, 13, 38, 39, 43
SHA	02, 09, 14, 21, 26, 30, 31,
PVG	03, 04, 10, 11, 15, 16, 22, 23, 27, 28, 32, 33, 34, 35
WUX	05, 17, 24, 40, 41
HGH	06, 12, 18, 20, 36, 42
NGB	07, 19, 25, 29, 37

This study utilized flight data from six prominent airports, NKG, SHA, PVG, WUX, HGH and NGB, in the Yangtze River Delta region. The dataset encompassed a two-hour period on a high-traffic day, specifically from 17:00:00 to 19:00:00, comprising a total of 165 flights. The model input data are the starting waypoint (EP) of all arrival flights into the airport metropolex area, and the corresponding entry time. All alternative arrival routes, segments and waypoints are known, along with the minimum flying duration for each segment.

### 3.2. Model Verification

In order to simplify the simulation model, since the routes of departing flights and arriving flights rarely overlap, only the sequencing of arrival flights is considered. In this experimental study, the optimization of the solution was conducted using Gurobi 10.0 solver and Python 3.9 interface programming, implemented on a 2.4 GHz i9-12900 CPU. The optimization process involved setting the MPS to five, considering the controller

workload, and T0 to zero. Notably, when encountering a shared waypoint, with the runway being considered as a specialized waypoint, specific safety intervals were established:  $T_{ij}$  was 60 s for radar-guided guidance,  $S_{ij}$  was 108 s for landing on the same runway, and  $s_{ij}$  was 48 s for landing on adjacent runways, according to the research results on the safety interval of parallel runway [23]. The rolling time domain algorithm's iterative process for the initial and final time domain datasets lacked the presence of data intervals both preceding and succeeding the time domain, which consequently resulted in disparities between the calculated outcomes and actual data. Therefore, for comparative purposes, our analysis was confined to data processing results within the second to penultimate time domains.

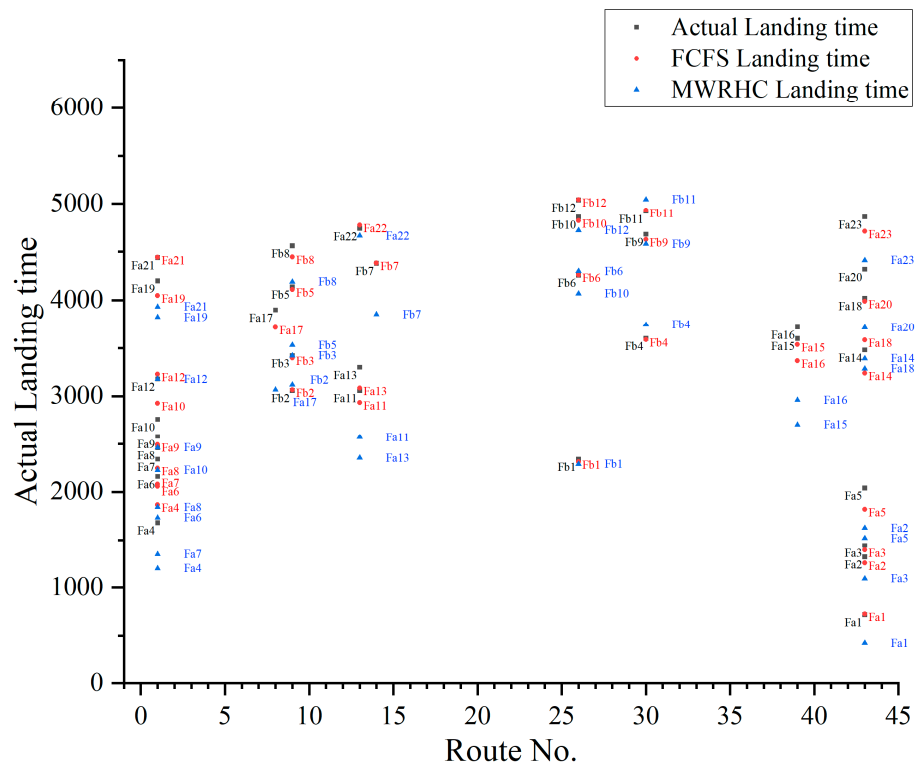
The solution results of actual, FCFS and the WMRHC model in this paper were compared, as shown in Table 8. Detailed insights into the chosen routes and landing sequences can be observed in Figure 4.

**Table 8.** (A) Comparison of model solution results for airport NKG. (B) Comparison of model solution results for airport SHA. (C) Comparison of model solution results for airport PVG. (D) Comparison of model solution results for airport WUX, HGH and NGB.

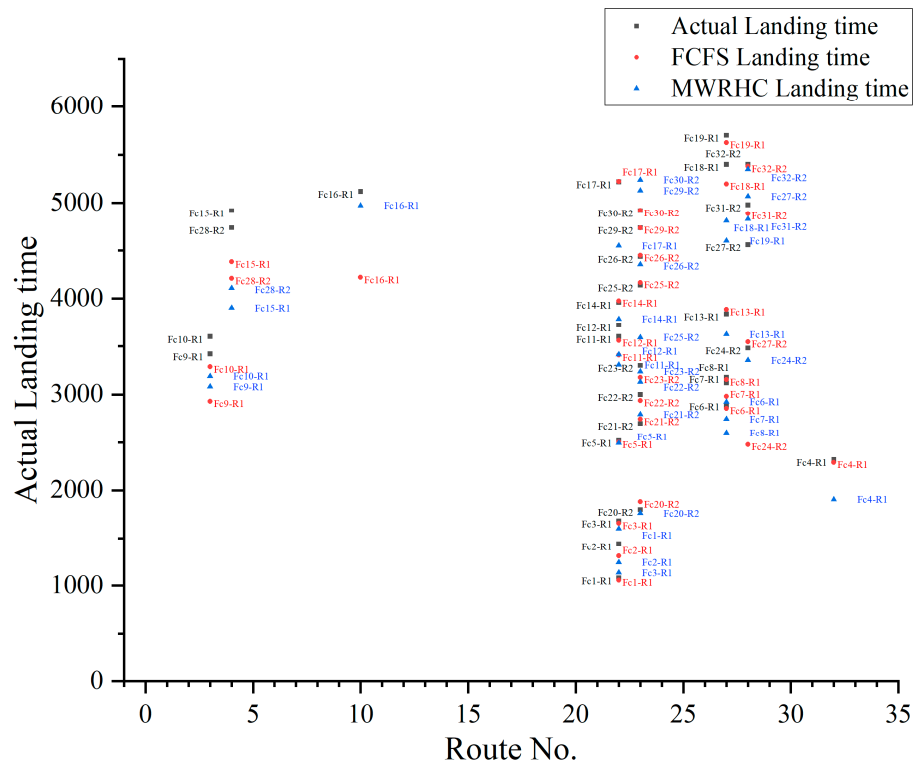
(A)									
Flight No.	Destination Airport	Landing Runway	Passing Time of EP	EP No.	Scheduled Landing Time	Actual Landing Time	FCFS Landing Time	MWRHC Landing Time	Route No.
Fa1	NKG	NKGR	125	S9	2400	720	725	425	43
Fa2	NKG	NKGR	655	S9	3000	1320	1255	1625	43
Fa3	NKG	NKGR	792	S9	2400	1440	1392	1092	43
Fa4	NKG	NKGR	103	S1	3900	1680	1867	1200	01
Fa5	NKG	NKGR	1217	S9	1800	2040	1817	1517	43
Fa6	NKG	NKGR	292	S1	2700	2160	2056	1733	01
Fa7	NKG	NKGR	124	S1	3300	2340	2080	1346	01
Fa8	NKG	NKGR	291	S1	300	2460	2247	1841	01
Fa9	NKG	NKGR	729	S1	1800	2580	2493	2462	01
Fa10	NKG	NKGR	1162	S1	4800	2760	2926	2227	01
Fa11	NKG	NKGR	993	S3	5100	3060	2933	2570	13
Fa12	NKG	NKGR	1465	S1	3300	3180	3229	3177	01
Fa13	NKG	NKGR	1146	S3	3000	3300	3086	2354	13
Fa14	NKG	NKGR	2640	S9	3900	3480	3240	3393	43
Fa15	NKG	NKGR	1924	S8	5400	3600	3536	2705	39
Fa16	NKG	NKGR	1756	S8	5700	3720	3368	2960	39
Fa17	NKG	NKGR	1673	S2	4200	3900	3717	3068	08
Fa18	NKG	NKGR	2985	S9	3300	4020	3585	3285	43
Fa19	NKG	NKGR	2284	S1	2100	4200	4048	3825	01
Fa20	NKG	NKGR	3391	S9	5100	4320	3991	3717	43
Fa21	NKG	NKGR	2679	S1	4500	4440	4443	3933	01
Fa22	NKG	NKGR	2832	S3	5400	4740	4772	4663	13
Fa23	NKG	NKGR	4111	S9	6600	4860	4711	4411	43
(B)									
Flight No.	Destination Airport	Landing Runway	Passing time of EP	EP No.	Scheduled landing time	Actual landing time	FCFS landing time	MWRHC landing time	Route No.
Fb1	SHA	SHAR	252	S6	3000	2340	2312	2289	26
Fb2	SHA	SHAR	321	S2	3900	3060	3065	3121	09
Fb3	SHA	SHAR	853	S2	3600	3420	3397	3422	09
Fb4	SHA	SHAR	1707	S7	3300	3600	3587	3746	30
Fb5	SHA	SHAR	1467	S2	4500	4140	4111	3530	09
Fb6	SHA	SHAR	2403	S6	4200	4260	4263	4299	26
Fb7	SHA	SHAR	1974	S3	6600	4380	4382	3854	14
Fb8	SHA	SHAR	1903	S2	5400	4560	4447	4191	09
Fb9	SHA	SHAR	2746	S7	6300	4680	4626	4580	30
Fb10	SHA	SHAR	2660	S6	6000	4860	4820	4070	26
Fb11	SHA	SHAR	3051	S7	5400	4920	4931	5044	30
Fb12	SHA	SHAR	2781	S6	6000	5040	5041	4720	26

Table 8. Cont.

(C)									
Flight No.	Destination Airport	Landing Runway	Passing time of EP	EP No.	Scheduled landing time	Actual landing time	FCFS landing time	MWRHC landing time	Route No.
Fc1	PVG	PVGR1	6	S5	3300	1080	1058	1599	22
Fc2	PVG	PVGR1	160	S5	2400	1440	1312	1244	22
Fc3	PVG	PVGR1	603	S5	2100	1680	1655	1136	22
Fc4	PVG	PVGR1	307	S7	3300	2320	2291	1906	32
Fc5	PVG	PVGR1	1450	S5	3900	2520	2502	2494	22
Fc6	PVG	PVGR1	794	S6	3600	2880	2858	2926	27
Fc7	PVG	PVGR1	916	S6	3000	3120	2980	2746	27
Fc8	PVG	PVGR1	1090	S6	5100	3180	3154	2603	27
Fc9	PVG	PVGR1	415	S1	2400	3420	2931	3082	03
Fc10	PVG	PVGR1	770	S1	5400	3600	3286	3190	03
Fc11	PVG	PVGR1	2255	S5	2100	3600	3407	3306	22
Fc12	PVG	PVGR1	2407	S5	6900	3720	3559	3414	22
Fc13	PVG	PVGR1	1822	S6	5400	3840	3886	3622	27
Fc14	PVG	PVGR1	2824	S5	5700	3960	3976	3786	22
Fc15	PVG	PVGR1	2059	S1	6000	4920	4833	3903	04
Fc16	PVG	PVGR1	2116	S2	6600	5120	4220	4974	10
Fc17	PVG	PVGR1	4071	S5	6900	5220	5223	4550	22
Fc18	PVG	PVGR1	2934	S6	5700	5400	5198	4813	27
Fc19	PVG	PVGR1	3360	S6	5400	5700	5624	4602	27
Fc20	PVG	PVGR2	728	S5	4800	1800	1880	1760	23
Fc21	PVG	PVGR2	1593	S5	3600	2700	2745	2794	23
Fc22	PVG	PVGR2	1786	S5	6900	3000	2938	3130	23
Fc23	PVG	PVGR2	2026	S5	3300	3300	3178	3238	23
Fc24	PVG	PVGR2	1215	S6	4200	3480	2479	3354	28
Fc25	PVG	PVGR2	3015	S5	5700	4140	4167	3592	23
Fc26	PVG	PVGR2	3297	S5	6300	4440	4449	4356	23
Fc27	PVG	PVGR2	2282	S6	4500	4560	3546	5068	28
Fc28	PVG	PVGR2	1693	S1	6600	4740	4209	4108	04
Fc29	PVG	PVGR2	3585	S5	4800	4740	4737	5128	23
Fc30	PVG	PVGR2	3767	S5	7200	4920	4919	5240	23
Fc31	PVG	PVGR2	2525	S6	6000	4980	4889	4832	28
Fc32	PVG	PVGR2	3076	S6	5100	5400	5380	5348	28
(D)									
Flight No.	Destination Airport	Landing Runway	Passing time of EP	EP No.	Scheduled landing time	Actual landing time	FCFS landing time	MWRHC landing time	Route No.
Fd1	WUX	WUXR	126	S3	3000	2100	1690	1238	17
Fd2	WUX	WUXR	541	S1	5700	3300	3173	2860	05
Fd3	WUX	WUXR	3452	S5	7200	5400	4608	4468	24
Fd4	WUX	WUXR	4445	S5	9900	6360	5601	5334	24
Fe1	HGH	HGHR	220	S8	2100	780	1064	670	42
Fe2	HGH	HGHR	404	S8	2400	1260	1248	854	42
Fe3	HGH	HGHR	610	S8	3300	1560	1454	1060	42
Fe4	HGH	HGHR	927	S8	2400	1860	1771	1377	42
Fe5	HGH	HGHR	1606	S8	4200	2460	2450	2056	42
Fe6	HGH	HGHR	1943	S8	2700	2880	2843	2439	42
Fe7	HGH	HGHR	2754	S8	4500	3600	3654	3309	42
Fe8	HGH	HGHR	3056	S8	5400	3780	3900	4639	42
Fe9	HGH	HGHR	1265	S2	5400	3960	2961	2620	12
Fe10	HGH	HGHR	3404	S7	4500	4260	4220	4126	36
Fe11	HGH	HGHR	1875	S1	5100	4380	3783	3417	06
Fe12	HGH	HGHR	4081	S8	6000	4920	4925	4531	42
Fe13	HGH	HGHR	2702	S4	5700	5040	4810	5235	20
Ff1	NGB	NGBR	15	S7	3600	1380	1251	1016	37
Ff2	NGB	NGBR	668	S6	2700	1920	1720	1466	29
Ff3	NGB	NGBR	481	S5	2700	2340	1889	2530	25
Ff4	NGB	NGBR	1347	S6	3000	2940	2399	1979	29
Ff5	NGB	NGBR	1491	S6	3900	3180	2543	2206	29
Ff6	NGB	NGBR	956	S5	1500	3360	2364	2314	25
Ff7	NGB	NGBR	1259	S5	2700	3540	2667	2422	25
Ff8	NGB	NGBR	1082	S5	3300	3720	2490	2098	25
Ff9	NGB	NGBR	494	S3	4500	3960	3354	2900	19
Ff10	NGB	NGBR	2160	S6	5100	4140	3212	2792	29
Ff11	NGB	NGBR	3210	S7	5400	4620	4446	4011	37
Ff12	NGB	NGBR	3516	S7	6000	4860	4752	4459	37

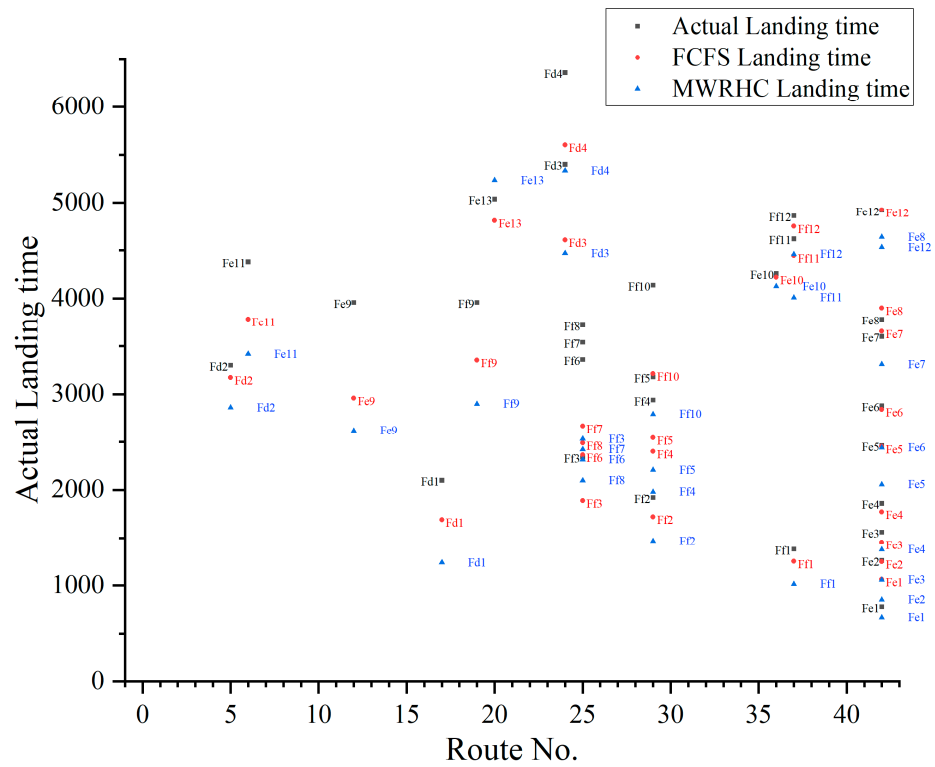


(a) Flights landing at airports NKG and SHA.



(b) Flights landing at airport PVG (2 runways for landing).

Figure 4. Cont.



(c) Flights landing at airports WUX, HGH and NGB.

Figure 4. Comparison of flight landing sequence and landing time.

In Table 8, “Flight No.,” “Destination Airport,” “Passing time of EP” and “EP No.” are the inputs, “Scheduled landing time” is the landing time in flight schedule, “Actual landing time” is the landing time of actual time, “FCFS landing time” and “MWRHC landing time” are simulated results according to the corresponding algorithm. “Landing Runway” and “Route No.” are the results obtained during the calculation of MWRHC, since the flight entering through an EP could have more than one route or runway to choose from.

To illustrate the data more effectively, we used the dataset from Nanjing Airport as a reference. Figure 5 offers a graphical representation comparing the FCFS-optimized landing times to those optimized using the MWRHC algorithm for flights at Nanjing Airport. The *x*-axis denotes the FCFS optimized landing durations in seconds, while the *y*-axis showcases the MWRHC optimized landing durations, also measured in seconds.

Unique markers indicate the actual landing times: square markers for FCFS and circular markers for MWRHC. Linear fits for each set of landing times are depicted—the red line for FCFS and the purple line for MWRHC.

The graph clearly reveals that MWRHC-optimized landing times frequently register below their FCFS counterparts. This suggests the superior efficiency of the MWRHC algorithm in trimming down overall landing durations when compared to the conventional FCFS approach.

Further, the curve for the MWRHC optimization consistently lies beneath the FCFS curve, emphasizing an improvement in average landing durations. The result reinforces the effectiveness of the MWRHC algorithm in both reducing landing times and refining the landing sequence of aircraft, in contrast to the prevailing real-world methods.

As the optimization algorithm fine-tunes the landing order of certain flights, a comparison of the optimization results solely based on the last landing flights within the time domain is inadequate. Consequently, to assess and compare the efficiency of the two algorithms, we introduced the concept of “saved flight time per flight”, which takes into account the overall time required for the optimization process. Actual landing time of flight *i* is represented by the symbol  $LT^{i}_{actual}$ , and the optimized landing time by FCFS

or MWRHC algorithm are denoted as  $LT_{FCFS}^i$  and  $LT_{MWRHC}^i$ , respectively. The “saved flight time per flight” of airport  $a$  can be expressed as  $c_a$ , which can be calculated by  $c_a = \sum_{i \in F_a} (LT_{MWRHC}^i (or LT_{FCFS}^i) - LT_{actual}^i) / N_a$  for airport  $a$ .

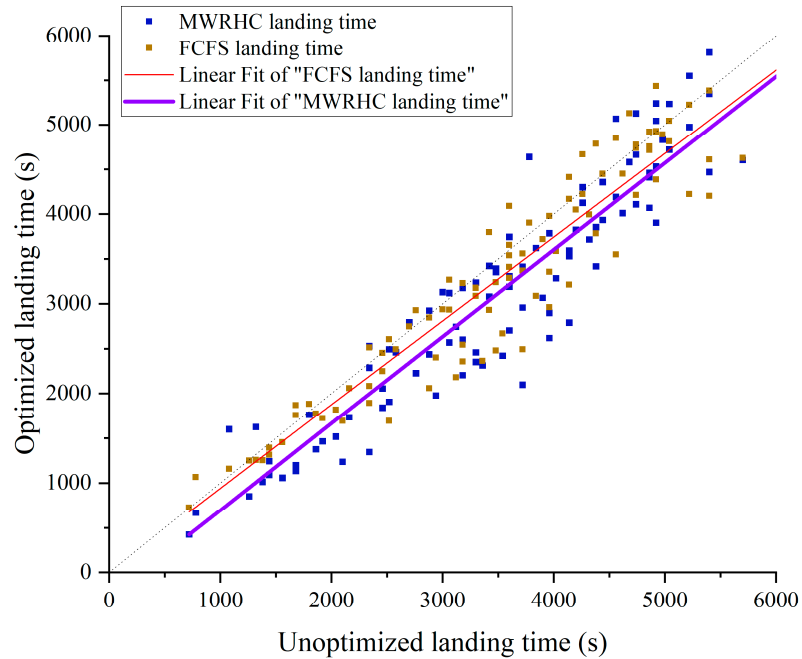


Figure 5. Comparison of landing times after optimized at Airport NKG.

Figure 6 presents the optimization time cost rate,  $c$ , of the six airports within the airport group following the application of two algorithms. The unit of measurement for  $c$  is seconds. The depicted values represent the average optimization time across multiple trials for each airport. A direct correlation exists between the magnitude of  $c$  and the efficiency of the optimization algorithm: higher  $c$  values suggest superior performance. Notably, the optimization effect of the MWRHC algorithm proves to be more effective in single-runway airports (WUX, HGH, NGB, NKG and SHA) compared to a dual-runway airport like PVG. For a detailed breakdown of the data represented in Figure 5, please refer to Table 8.

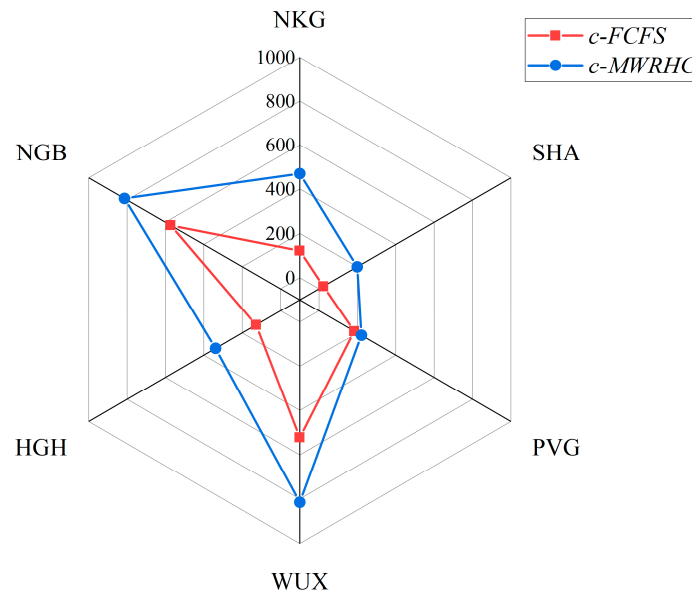


Figure 6. Comparison of the optimization time cost rate of six airports.

#### 4. Conclusions

This study focuses on the airport metroplex system and addresses the arrival sequencing problem involving multiple airports, multiple runways, and multiple routes within this system. To this end, a comprehensive MIP model is formulated, which integrates the various elements of the arrival optimization. By adopting the maximum landing efficiency as the objective function, the approach optimization control for multiple airports and runways is achieved while taking into account constraints such as crossing time intervals, route selection, and landing intervals.

The MWRHC algorithm is employed to tackle time-efficiency challenges in the multi-airport and multi-runway arrival flight scheduling model within an airport group. Notably, this algorithm incorporates a crucial safety feature by continuously monitoring the presence of flights within the terminal area, thus ensuring flight safety is maintained throughout the entire optimization process.

Utilizing actual flight data from a busy day in the Yangtze River Delta airport metroplex, the proposed model is employed to optimize the arrival flight sequencing. The optimization results demonstrate an improvement compared to the traditional FCFS algorithm, thus validating the effectiveness and efficacy of the proposed model algorithm.

The comparative analysis of the optimization outcomes for the six airports within the airport group indicates that the algorithm yields more favorable results in terms of optimization for single-runway airports compared to those with dual runways.

This research contributes to the upgrading of traditional decision support tools to provide a suggested sequence that accommodates the traffic condition in the airport metroplex area. In future work, the authors will extend this method to combined arrival and departure scheduling, multi-runway scheduling, and metroplex scenarios.

**Author Contributions:** Conceptualization, F.J. and Z.Z.; methodology, Z.Z.; data curation, F.J.; writing—original draft preparation, F.J.; writing—review and editing, F.J. and Z.Z. All authors have read and agreed to the published version of the manuscript.

**Funding:** This research was funded by the Key Projects of the Civil Aviation Joint Fund of the National Natural Science Foundation of China (Grant No. 2233209), as well as the Fundamental Research Funds for the Central Universities (Grant No. 3122022053).

**Data Availability Statement:** The data used to support the findings of this study are available from the corresponding author upon request.

**Conflicts of Interest:** The authors declare no conflict of interest.

#### References

1. FAA. Metroplex. Available online: [https://www.faa.gov/air\\_traffic/nas/metroplex](https://www.faa.gov/air_traffic/nas/metroplex) (accessed on 1 September 2023).
2. Donohue, G.; Hoffman, K.; Sherry, L.; Ferguson, J.; Qadar Kara, A. *Optimizing Air Transportation Service to Metroplex Airports: Part 1 Analysis of Historical Data*; NASA: Washington, DC, USA, 2010.
3. Donohue, G.; Hoffman, K.; Sherry, L.; Ferguson, J.; Qadar Kara, A. *Optimizing Air Transportation Service to Metroplex Airports: Part 2 Analysis Using the Airline Schedule Optimization Model (ASOM)*; NASA: Washington, DC, USA, 2010.
4. Ramanujam, V.; Balakrishnan, H. Estimation of arrival-departure capacity tradeoffs in multi-airport systems. In Proceedings of the Joint 48th IEEE Conference on Decision and Control and 28th Chinese Control Conference, Shanghai, China, 16–18 December 2009.
5. DeLaurentis, D.A.; Ayyalasomayajula, S. *Analysis of Dependencies and Impacts of Metroplex Operations*; NASA: Washington, DC, USA, 2010.
6. Donaldson, A.; Hansman, R.J. Capacity Improvement Potential for the New York Metroplex System. In Proceedings of the 10th AIAA Aviation Technology, Integration, and Operations (ATIO) Conference, Worth, TX, USA, 13–15 September 2010.
7. Jiang, F.; Zhang, Z.; Dai, X. Ground-Air Traffic Congestion Propagation Model Based on Hierarchical Control Interdependent Network. *J. Adv. Transp.* **2023**, *2023*, 4602148:1–4602148:22. [[CrossRef](#)]
8. Mesgarpour, M.; Potts, C.N.; Bennell, J.A. Models for Aircraft Landing Optimization. In Proceedings of the 4th International Conference on Research in Air Transportation (ICRAT 2010), Budapest, Hungary, 1–4 June 2010.
9. Hancerliogullari, G.; Rabadi, G.; Al-Salem, A.H.; Kharbeche, M. Greedy algorithms and metaheuristics for a multiple runway combined arrival-departure aircraft sequencing problem. *J. Air Transp. Manag.* **2013**, *32*, 39–48. [[CrossRef](#)]

10. Sölveling, G.; Clarke, J.-P. Scheduling of airport runway operations using stochastic branch and bound methods. *Transp. Res. Part C Emerg. Technol.* **2014**, *45*, 119–137. [[CrossRef](#)]
11. Ma, Y.; Hu, M.; Zhang, H.; Yin, J.N.; Wu, F. Optimized method for collaborative arrival sequencing and scheduling in metroplex terminal area. *Acta Aeronaut. Astronaut. Sin.* **2015**, *36*, 2279–2290.
12. Wang, L.; Gu, Q. Arrival and Departing Aircraft-sequencing Optimization under the Special Circumstances. *J. Transp. Systms Eng. Inf. Technol.* **2013**, *14*, 102–107.
13. Sidiropoulos, S.; Majumdar, A.; Han, K.; Schuster, W.; Ochieng, W.Y. A framework for the classification and prioritization of arrival and departure routes in Multi-Airport Systems Terminal Manoeuvring Areas. In Proceedings of the 15th AIAA Aviation Technology, Integration, and Operations Conference, Dallas, TX, USA, 22–26 June 2015.
14. Zhang, Z.; Wang, D. Research on flow allocation strategy based on capacity matching for airport group. *Mod. Electron. Tech.* **2019**, *42*, 113–116+120.
15. Yin, J.; Ma, Y.; Tian, W.; Chen, D.; Hu, Y.; Ochieng, W. Impact Analysis of Demand Management on Runway Configuration in Metroplex Airports. *IEEE Access* **2020**, *8*, 66189–66212. [[CrossRef](#)]
16. Liu, J.; Jiang, H.; Dong, X.; Lan, S.; Wang, H. Dynamic collaborative sequencing method for arrival flights based on air traffic density. *Acta Aeronaut. Astronaut. Sin.* **2020**, *41*, 323717.
17. Wang, L.; Lin, Y. Aircraft Sequencing Modeling and Algorithm for Shared Waypoints in Airport Group. *J. Transp. Inf. Saf.* **2021**, *39*, 93–99+136.
18. Sun, B.; Wei, M. An Optimization Model for Inbound and Outbound Flight Scheduling with Consideration of Runway Incursions. *Ind. Eng. Manag.* **2022**, *27*, 16–21.
19. Wei, M.; Wu, W.; Sun, B. An Optimization Model for Inbound and Outbound Flight Scheduling with Consideration of Potential Risk Levels and Priorities. *Ind. Eng. Manag.* **2022**, *27*, 40–45.
20. Faye, A. Solving the Aircraft Landing Problem with time discretization approach. *Eur. J. Oper. Res.* **2015**, *242*, 1028–1038. [[CrossRef](#)]
21. Pawełek, A.; Lichota, P.; Dalmau, R.; Prats, X. Fuel-Efficient Trajectories Traffic Synchronization. *J. Aircr.* **2019**, *56*, 481–492. [[CrossRef](#)]
22. Pawełek, A.; Lichota, P. Arrival air traffic separations assessment using Maximum Likelihood Estimation and Fisher Information Matrix. In Proceedings of the 2019 20th International Carpathian Control Conference (ICCC), Kraków, Poland, 26–29 May 2019; pp. 1–6.
23. Le, M.; Wu, X.; Hu, Y. Arrival Flights Optimal Sequencing Based on Path Selection and Rolling Horizon Control. *J. Beijing Univ. Aeronaut. Astronaut.* **2022**, *2022*, 1–11. [[CrossRef](#)]

**Disclaimer/Publisher’s Note:** The statements, opinions and data contained in all publications are solely those of the individual author(s) and contributor(s) and not of MDPI and/or the editor(s). MDPI and/or the editor(s) disclaim responsibility for any injury to people or property resulting from any ideas, methods, instructions or products referred to in the content.